

A modular PC based silicon microstrip beam telescope with high speed data acquisition

J. Treis^{a,1}, P. Fischer^a, H. Krüger^a, L. Klingbeil^a, T. Lari^b,
N. Wermes^a

^a*Physikalisches Institut der Universität Bonn, Germany*

^b*Dipartimento di Fisica di Università di milano e INFN, Sezione di Milano, Italy*

Abstract

A PC based high speed silicon microstrip beam telescope consisting of several independent modules is presented. Every module contains an AC-coupled double sided silicon microstrip sensor and a complete set of analog and digital signal processing electronics. A digital bus connects the modules with the DAQ PC. A trigger logic unit coordinates the operation of all modules of the telescope. The system architecture allows easy integration of any kind of device under test into the data acquisition chain.

Signal digitization, pedestal correction, hit detection and zero suppression are done by hardware inside the modules, so that the amount of data per event is reduced by a factor of 80 compared to conventional readout systems. In combination with a two level data acquisition scheme, this allows event rates up to 7.6 kHz. This is a factor of 40 faster than conventional VME based beam telescopes while comparable analog performance is maintained achieving signal to noise ratios of up to 70:1.

The telescope has been tested in the SPS testbeam at CERN. It has been adopted as the reference instrument for testbeam studies for the ATLAS pixel detector development.

1 Introduction

For the testing of newly developed detector systems, testbeam facilities are suitable and frequently used. They create experimental conditions which are closer to a high energy physics experiment than the conditions in the laboratory while permitting access to important experimental parameters. In order

¹ Corresponding author. Tel. +49 228 732499, fax. +49 228 733220, e-mail treis@physik.uni-bonn.de.

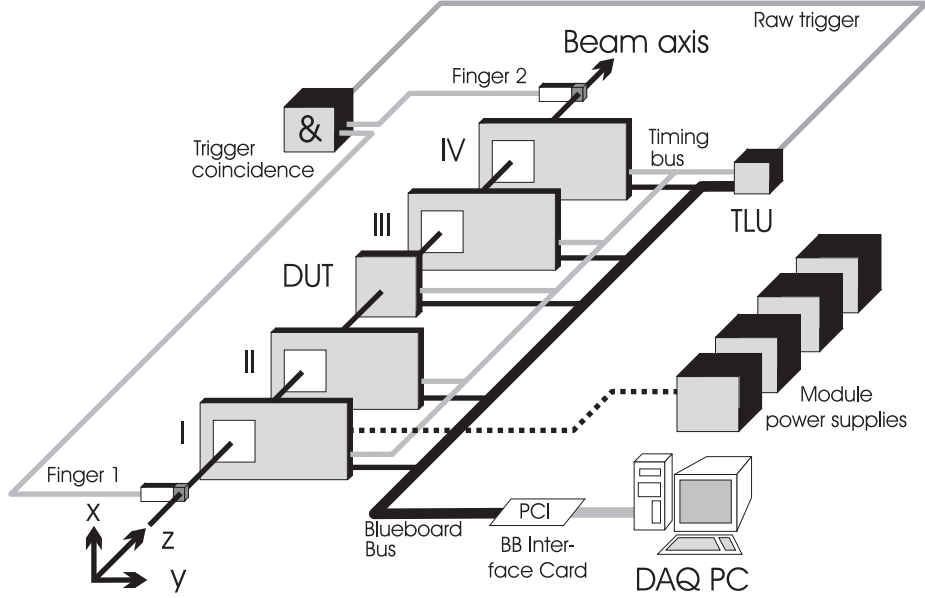


Fig. 1. A BAT beam telescope setup with four BAT modules and one BB based DUT.

to measure properties like efficiency and spatial resolution of a device under test (DUT), a precise reference measurement of the incident particle tracks is required. This is the task for a *beam telescope* [1,2,3] measuring intercept and angle for incident particles on an event by event basis. In order to achieve position resolutions in the μm and μrad scale silicon microstrip detectors are commonly used for such telescopes, providing a number of space points for track interpolation. Such microstrip based telescope systems suffer from limited event rate due to their large number of readout channels and their system architecture. Additionally, to synchronize such a system is difficult, and merging a given DUT readout into the system's data acquisition (DAQ) is a major task.

As beam time is often limited, speed is also an important requirement for a telescope system, especially when semiconductor detector devices with a structure size in the μm scale, for instance ATLAS pixel devices, are to be tested. The time needed to collect a significant number of events for every sensor element strongly depends on the readout speed of the telescope, as the DUT readout is very fast.

In this paper, the concept of a fully PC-based beam telescope system, henceforth referred to as BAT², is presented, which combines good track measurement accuracy with high event rate and easy DUT integration.

² An acronym for *Bonn ATLAS Telescope*.

2 System overview

Figure 1 shows a typical BAT setup consisting of four detector modules, a trigger logic unit (TLU), the data acquisition PC and a DUT. All components are connected via the purely digital "blueboard bus" (BB) [8]. Furthermore, the "timing bus" connects BAT modules, DUT and TLU.

A raw trigger signal indicating an event is provided by the coincidence of two scintillation counters. The coincidence signal is fed into the TLU, which then decides if a trigger is to be given according to the module's status information accessible on the timing bus. If so, the TLU generates the trigger signal and distributes it to the modules.

After receiving a trigger, each module acquires, digitizes and preprocesses event data autonomously and independent from an external sequencer logic. The event data is stored in a module-internal memory. When a certain amount of data is accumulated in a module's memory, the corresponding module alerts the data acquisition PC to read the entire data memory content of this module.

The DAQ processes running on the PC collect all data from the different modules, assemble the data which belong to one event and store it on the hard disk. Part of the data is processed, the results are made available to the user for monitoring purposes.

Several ways of integrating a DUT are feasible. The DUT can be connected directly to the BB, as shown in figure 1. For this purpose, a flexible BB interface is available. For integration of a given VME based DUT and supplementary measurement equipment, a VME crate can be attached to the DAQ PC using a commercially available PC to VME interface. And in case an embedded PC or a VME CPU is to be used for DAQ, a BB to VME interface has been developed for fully VME based operation of the entire telescope.

3 Module hardware

A BAT module consists of a sensor assembly, an analog telescope card (ATC) and a digital telescope card (DTC). An overview over a module's constituents and their interconnection is given in figure 2. A photograph of a fully assembled module is shown in figure 3.

The sensor assembly consists of the sensor and 2×5 front end ICs. The sensor is a commercially available double sided, AC-coupled silicon strip detector type S6934 with integrated polysilicon bias resistors manufactured by Hamamatsu photonics [4]. The n-side strips are isolated by p^+ -stop implantations. Implant and readout strip pitch are $50 \mu\text{m}$ on both sides, the nominal stereo angle is 90° . The sensitive area is $3.2 \times 3.2 \text{ cm}^2$ corresponding to 640 strips on each side.

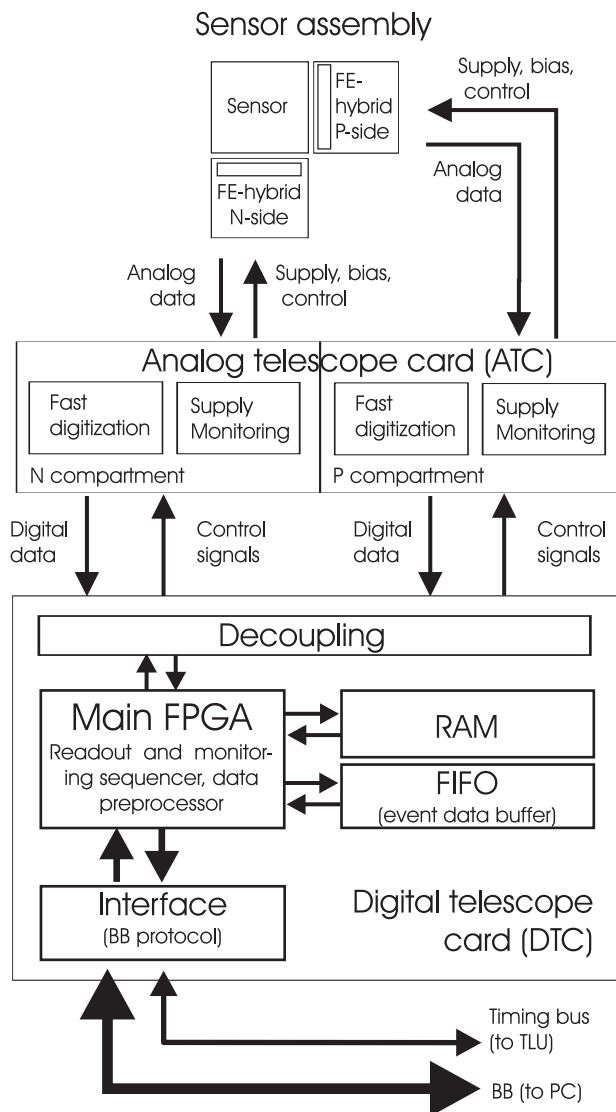


Fig. 2. Schematic layout of a BAT module.

The front end IC used is the VA2 manufactured by IDE AS, Oslo [5]. The VA2 is a 128 channel charge sensitive preamplifier-shaper circuit with simultaneous sample and hold, serial analog readout and calibration facilities. Five VA2 ICs are needed to provide readout for one detector side. They are mounted on a so-called BELLE hybrid [6,7], a ceramic carrier with an attached PCB providing support for the VAs and distributing supply, bias and digital control to them. As VAs on the hybrid are operated in a *daisy chain*, a hybrid is read out like one large 640 channel VA. Sensor and hybrids are fixed to a ceramic support structure, which is attached to a solid aluminum frame for handling. The ATC is divided into two identical compartments supporting one BELLE hybrid each. A hybrid's compartment provides the supply voltages, bias voltages and bias currents required by the hybrid. A fast ADC circuit is used for digitization of the VA2 output data, and an additional multi-channel ADC al-

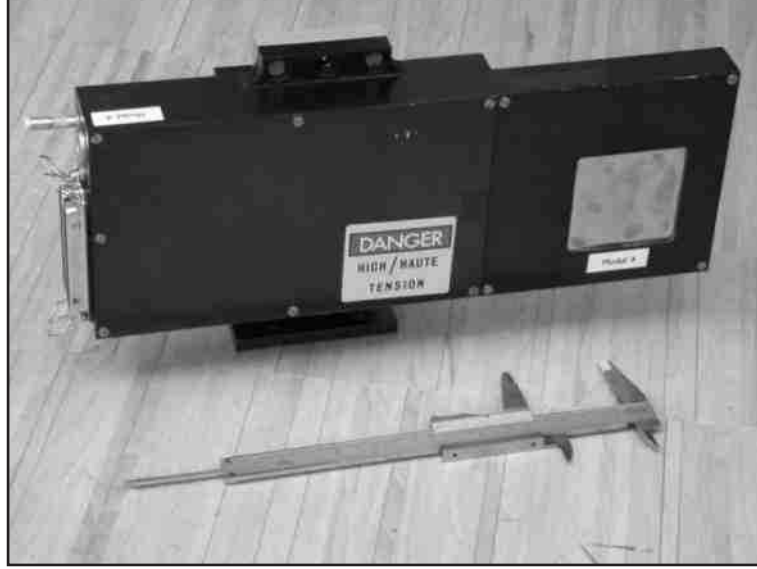


Fig. 3. Photo of a BAT module.

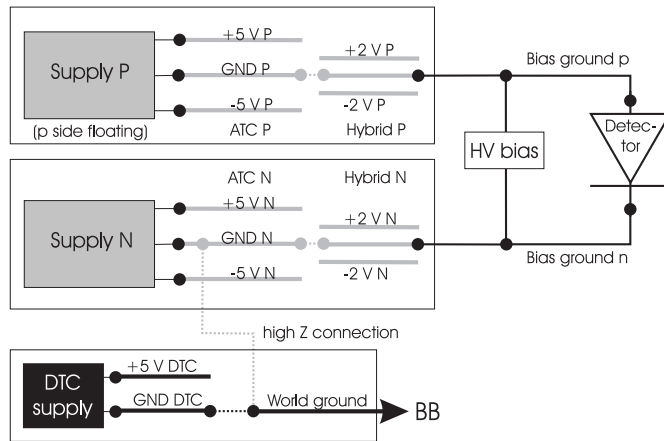


Fig. 4. Powering and grounding scheme of a telescope module.

allows observation of the most important hybrid parameters during operation. Only digital signals are transferred between ATC and DTC via digital couplers. The central functional building block of the DTC is the *readout sequencer*. Implemented into the *main FPGA*, this circuit generates the control sequence needed to acquire and digitize the analog FE data. Both hybrids are read out simultaneously. The readout sequencer also controls the *data preprocessing logic*. Furthermore, the DTC holds a large FIFO for on-module data buffering and a RAM for storing data preprocessing information. A second FPGA circuit controls access to the BB and the timing bus. It is also capable of sending interrupt requests (IRQs) on the BB to the PC. Each module has its own power supply, providing three independent voltage sources needed to operate the ATC compartments and the DTC. The power supply also generates the detector bias voltage. The powering and grounding scheme of a telescope module is shown in figure 4.

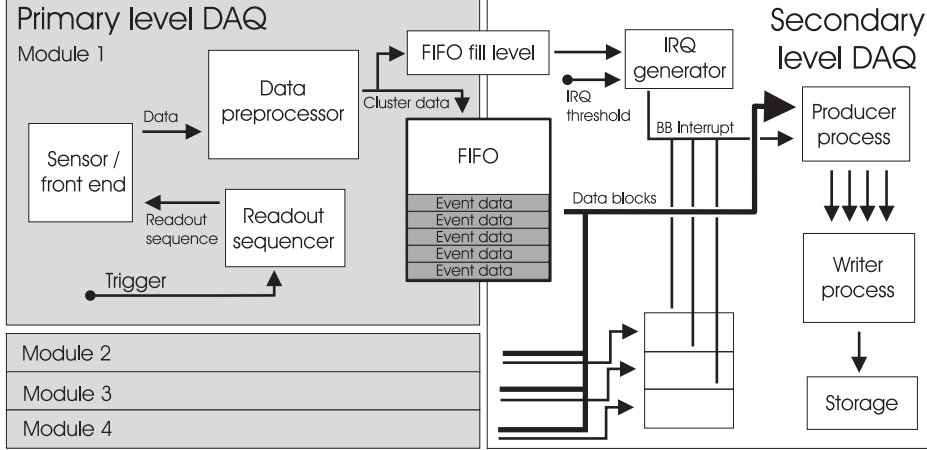


Fig. 5. Structure of the telescope DAQ.

4 Data acquisition

4.1 Structure

The data acquisition of the BAT is implemented as a two-level process. The primary level DAQ (DAQ I), controlled by the readout sequencers in every module, is simultaneously performed inside each module directly after receiving a trigger signal. The secondary level DAQ (DAQ II) is PC controlled and common for all modules. Both DAQ levels running independently reduces the effective system dead time to the DAQ I runtime (see also section 5). The telescope DAQ structure is shown in figure 5. An example for DAQ I and DAQ II interaction is shown in figure 6.

4.2 Primary level DAQ: Digitizing and preprocessing

When receiving a trigger, a module's readout sequencer acquires and digitizes the data residing in the front end ICs and operates the data preprocessing logic, which performs pedestal correction, hit detection and zero suppression. Pedestal correction is done by subtracting an individual pedestal value for each channel. Hits are detected by applying an individual threshold to the pedestal corrected data. Pedestal and threshold values have to be determined and stored beforehand in the DTC RAM. Zero suppression is done by storing only *clusters* consisting of the information of the 5 neighboring channels around the hit channel in the DTC FIFO. Enlarged clusters are stored for two or more hit channels in close proximity. Multiple clusters per event are possible. The data volume for an event with one hit cluster is 32 byte in total. Compared to a typical event size of 2.5 kByte for common telescope systems

[2], the amount of data is reduced by a factor 1/80.

After finishing preprocessing an event, end of event data (EOD) is written to the FIFO, which transmits a module internal trigger number count and the so-called common mode count (CMC) value. The CMC value is used to calculate and correct the common mode fluctuation amplitude for this event in on- or offline analysis. DAQ I has finished processing an event as soon as a complete module event data block (MED) including cluster data and EOD has completely been written to the FIFO.

4.3 Secondary level DAQ: Data readback and event building

While DAQ I is active, MEDs keep accumulating in the modules' FIFOs until a certain threshold fill level is exceeded. A module internal interrupt generator generates an IRQ, forcing DAQ II to become active.

DAQ II, responsible for data transfer to the PC, is controlled by the *producer* task, which runs on the data acquisition PC. It controls one *shared buffer*, a FIFO like structure in PC RAM, for every module. When detecting an IRQ from a certain module, the producer transfers the data from this module's buffer FIFO to the corresponding shared buffer. DAQ I operation is not affected by this data transfer and continues to process events. The *writer* software process collects and assembles MEDs belonging to the same event from the different shared buffers and stores them on the hard disk.

The modules' threshold fill level can be adjusted with respect to the beam intensity. A single event operation mode for low beam intensities is also available.

5 Trigger logic

As each module takes data autonomously, trigger control is necessary to prevent the trigger synchronization from getting lost. Every device is therefore connected to the trigger logic implemented in the TLU, receives its trigger signal from the TLU and has a dedicated busy line on the timing bus, which indicates DAQ I activity. The TLU generates a gate signal for the raw trigger from the coincidence of all devices' busy signals, which only sends triggers if all devices are not busy. The system's dead time is therefore determined by the busy signal from the slowest device. The timing of gate and busy signals is shown in figure 6.

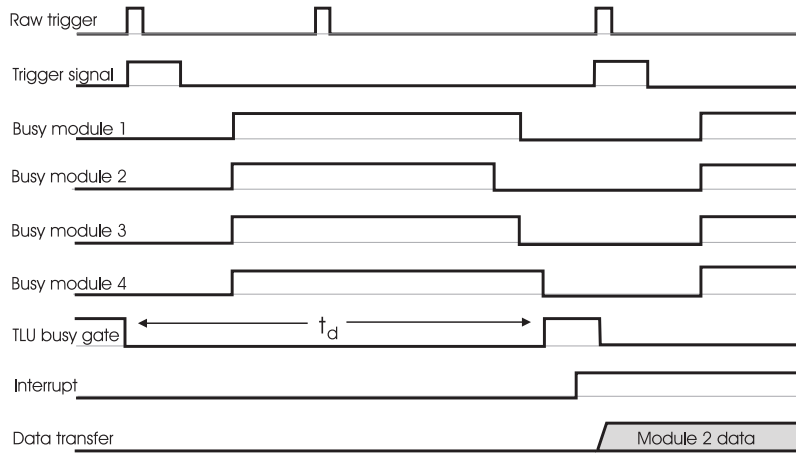


Fig. 6. Example for TLU, DAQ I and DAQ II timing. In this example, module 2 generates an IRQ right after the first event was fully processed. The producer starts the data transfer immediately afterwards, while DAQ I processes the second event.

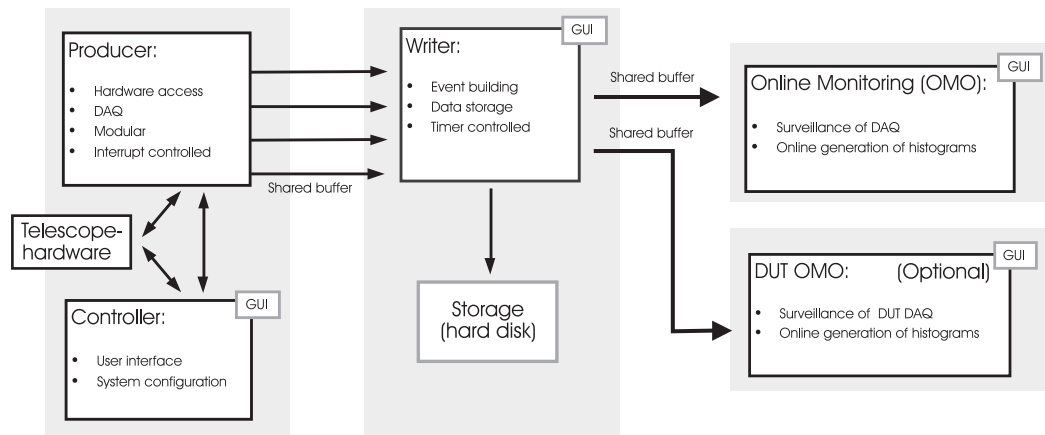


Fig. 7. Structure of the BATDAQ software package. The online monitoring (OMO) process allows monitoring of telescope module data. The DUT OMO is responsible for monitoring of DUT data.

6 Software

The DAQ PC is a commercial PC equipped with a dual Pentium II processor running the Windows NT 4.0 operating system and the DAQ software package written in C++. It is connected to the BB via a BB to PCI interface card [8]. In addition to the DAQ processes mentioned, online monitoring processes allow an overview about the device performance during operation. An overview over the different processes and their tasks is given in figure 7.

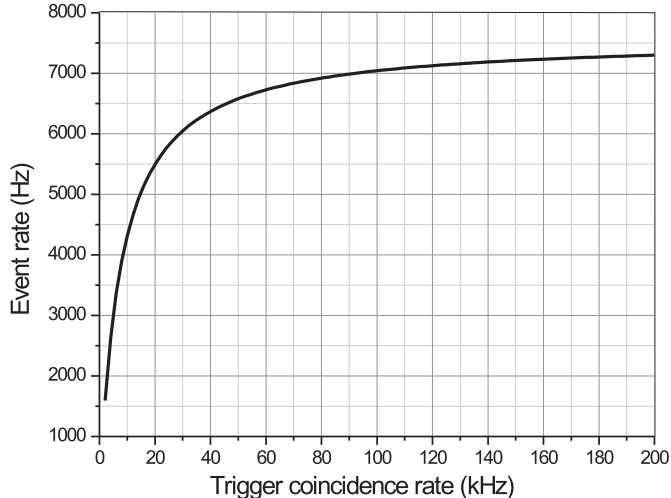


Fig. 8. Dependency of event rate on trigger coincidence rate.

7 System performance

7.1 Event rate

The mean event rate of the telescope system is determined by the dead time of the slowest device, being the BAT modules in most applications due to their serial readout. A BAT module's dead time t_{dt} is dominated by the DAQ I runtime³, which is 132 μ s. The event rate actually observed also depends on the trigger coincidence rate Φ_T , and is given by:

$$\frac{1}{v_e^{max}} = t_{dt} + \frac{1}{(1 - e^{-\Phi_T})} \quad (1)$$

assuming Poisson statistics. The dependence of event rate and trigger coincidence rate is shown in figure 8. At the H8 testbeam at CERN, a system consisting of 4 BAT modules and one BB based DUT has been operated with an effective event rate of 4.5 kHz. This is an event rate larger than the event rate of conventional VME-based systems by factors of 40 [1] to 75 [2].

7.2 Analog performance

Figure 9 shows a hit map and source profiles of a ^{90}Sr β source scan using a PIN diode as trigger device. Only one dead channel on the N-side and a few

³ The readout sequencer has to read 640 channels with a serializer clock frequency of 5 MHz.

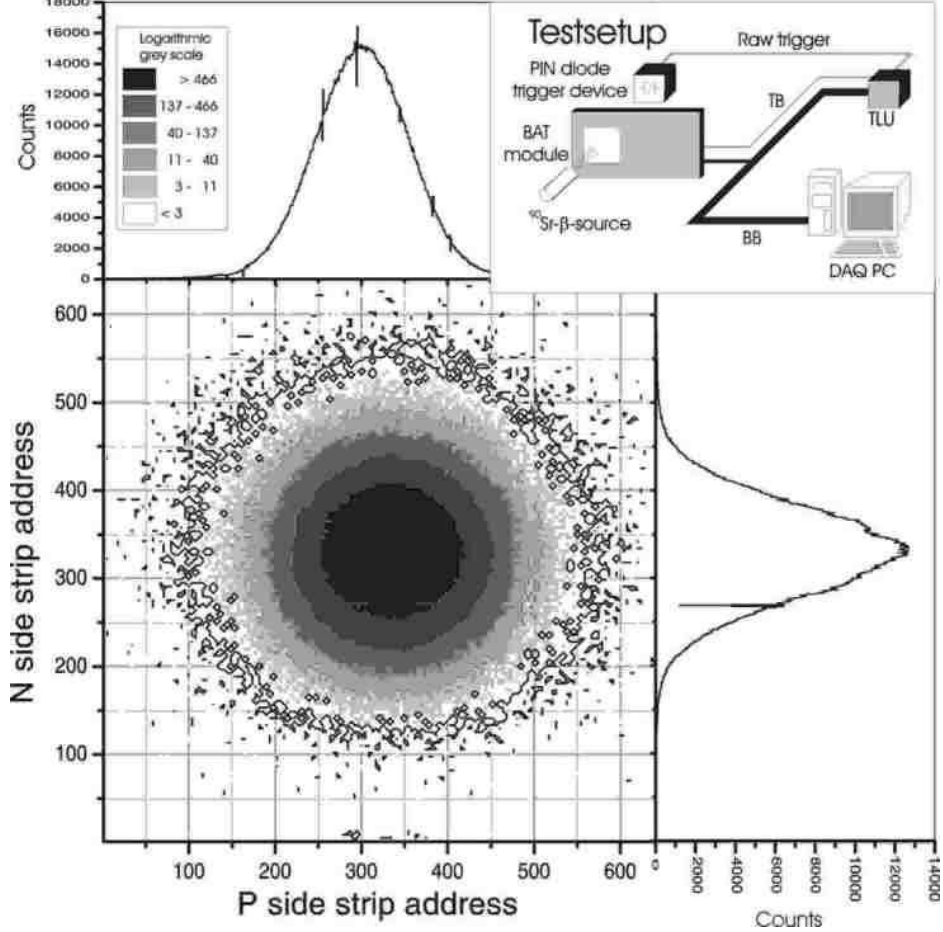


Fig. 9. Experimental setup, hit map and source profiles for N- and P- side for a source scan of a module using a ^{90}Sr β source with about 2500000 events. The number of entries in each bin is grey coded.

noisy channels on the P-side are observed. The system operates stably. No pedestal drift was observed during a 32-hour run. Thus taking pedestals only once at the beginning of each run is sufficient. Common mode noise is also tolerable.

Figure 10 shows a typical pulse height distribution together with the noise histogram of N- and P-side of the same module. One ADC count corresponds to an ENC of $20 e^-$ on P and $24 e^-$ on N-side, as can be calculated from the position of the peak in the respective pulse height distribution. Thus, the mean ENC value for all channels is $706 e^-$ for the N-side and $340 e^-$ for the P-side. Comparing these values with the most probable charge deposition for a minimal ionizing particle in $300 \mu\text{m}$ thick silicon, which is $23300 e^-$, yields signal to noise ratios of 33 for the N- and 69 for the P-side, which is comparable to the results obtained with other telescope systems [1,2,3]. Figure 11 shows the correlation between the pulse heights observed on N- and P- side of the detector for an event. The pulse height correlation can be used to solve strip data ambiguities, which can occur at high beam intensities.

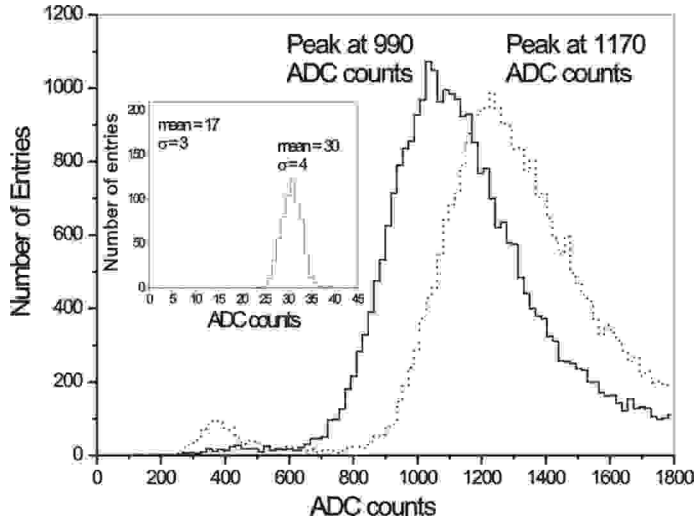


Fig. 10. Landau-shaped pulse height distributions of a module in a 70 GeV pion beam for N-side (solid line) and P-side (dashed line). The insert shows the channel noise histograms for the same module.

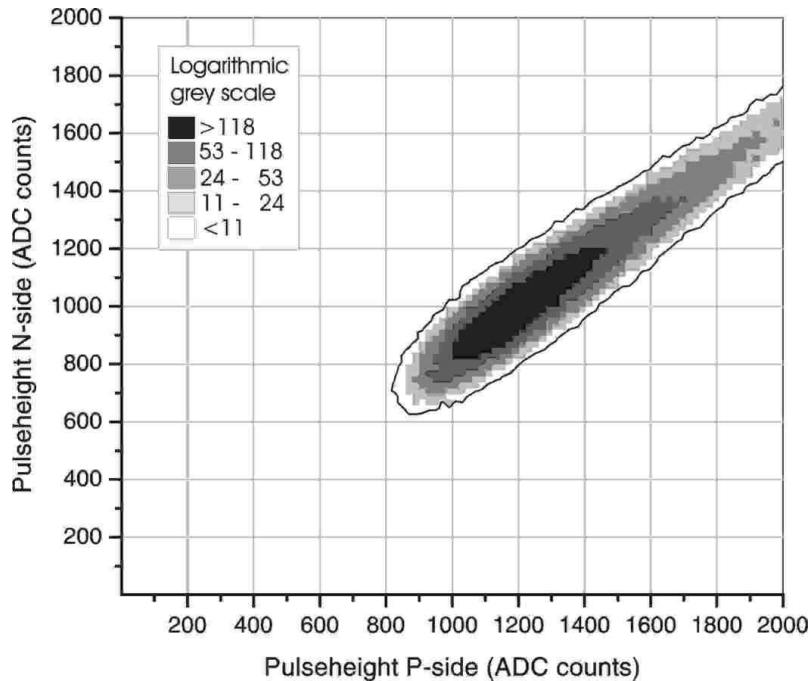


Fig. 11. Pulse height correlation between N- and P-side of the same detector module. The number of entries in each bin is grey coded.

Charge sharing between detector strips can be used for a more exact reconstruction of the position of a hit on a module, as the BAT provides analog cluster readout. The normalized pulse heights of the three central strips of a cluster can conveniently be displayed in the form of a *triangle plot* (figure 12). Using the different normalized amplitudes of the three central strips of a cluster as distances from the sides of an equilateral triangle, the triangle plot is a way to display the distribution of the signal charge among the three cen-

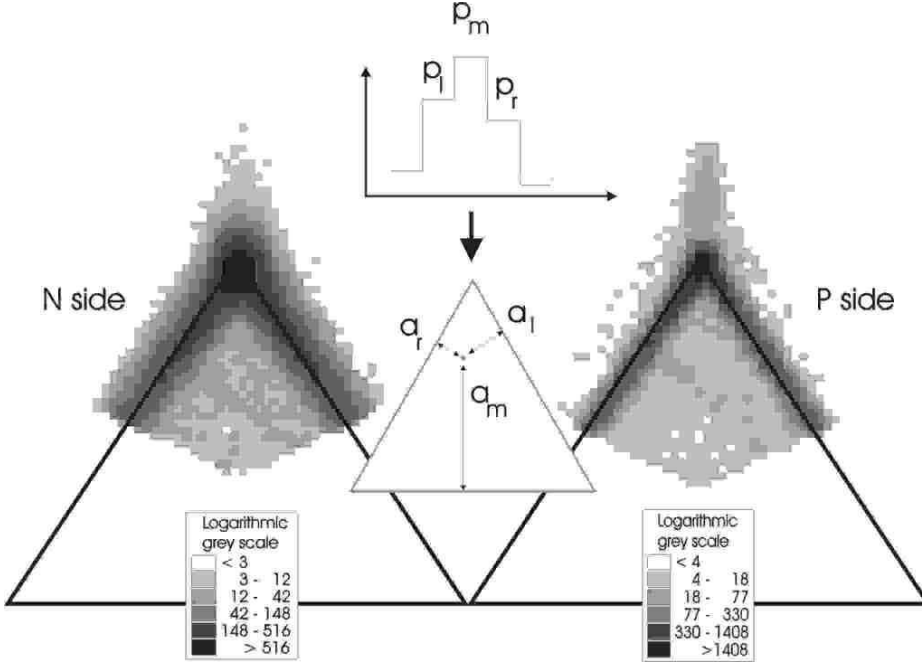


Fig. 12. Principle of a triangle plot and triangle plots for both detector sides of one module. The a_l , a_m , a_r are the p_l , p_m , p_r values normalized on the sum of the values. The number of entries in each bin is grey coded.

tral channels. Events in which most of the charge is deposited in the central cluster channel lie at the top of the triangle, events in which the charge is divided between two cluster channels lie on the sides of the triangle. Events with significant amounts of charge on all three central channels lie in the central area of the triangle. Entries outside the triangle area are due to "negative" signal amplitudes after pedestal subtraction caused by noise. In most cases the charge is deposited only in the central cluster strip or in two strips. Charge distribution over three or more channels, mostly due to δ -electrons, are rare; thus an algorithm using only two cluster charges for reconstruction is appropriate. The commonly used η -algorithm [9] uses the pulse heights of the two central cluster channels which carry the largest signals within the cluster:

$$\eta = \frac{c_1}{(c_1 + c_2)} \quad (2)$$

with c_1 , c_2 being the amplitude of the left and the right central cluster channel. Assuming a uniform distribution of hits and charge sharing independent from the total pulse height, the integral of the η -distribution can be used to calculate a position correction value Δx by

$$\Delta x(\eta) = \frac{p}{N_0} \int_0^\eta \frac{dN}{d\eta'} d\eta' \quad (3)$$

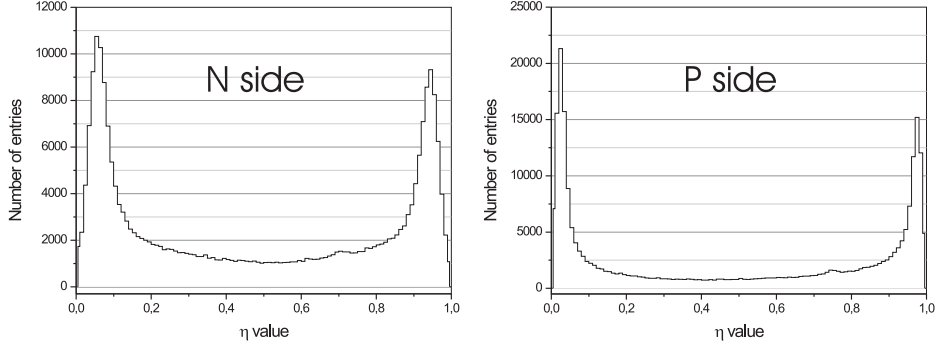


Fig. 13. Distributions of η for both detector sides.

with p being the strip pitch and N_0 the total number of entries in the η distribution histogram. The correction value is then added to a reference position to obtain the absolute position of the hit. Typical η distributions for a single module are displayed in figure 13. The differences in shape of the η distribution between N- and P- side are mostly due to different interstrip capacitances on the detector sides. The asymmetry of the distribution for one detector side is due to parasitic capacitances in the analog readout of the strips. They can be corrected by applying a deconvolution algorithm. Their influence on the spatial resolution of the detectors is, however, small.

7.3 Spatial resolution

The telescope tracking performance has been studied using test beam data taken with a 180 GeV/ c pion beam at the CERN H8 testbeam at the SPS. The raw event data is processed by a program developed by the Milano ATLAS group which performs event reconstruction and alignment of the telescope planes.

A straight line fit is applied to the strip hits, and the residuals between the hits and the fitted track are computed for the strip planes. Then, an analytical alignment algorithm is applied to the strip planes, which minimizes the residuals and their dependence on position and angle of the tracks. The alignment and the tilt angle are calculated for all strip planes using the first strip plane as reference plane. Examples of the resulting residual distributions for the strip planes in one direction after alignment are presented in figure 14, showing the quality of the alignment algorithm. The distributions are properly centered around zero, which indicates the absence of systematic errors. Their widths, which are determined by the intrinsic resolution of the strip planes, multiple scattering and the alignment algorithm, lie between 6.3 and 4.2 μm .

As the data from the strip planes, however, is used in the track fit, the width of the strip plane residuals can not be taken to determine the spatial resolution of the telescope. For this purpose, the residual distributions in the DUT planes have to be considered.

The telescope setup included two DUTs, which were hybrid pixel detectors. Sensor and front end electronics were developed by the ATLAS pixel collaboration [12,13]. The sensor has no inefficient area, the pixel cell size was $50 \mu\text{m} \times 400 \mu\text{m}$ corresponding to the pixel pitch, and the front end electronics provides for zero-suppressed readout, reporting both pixel position and charge deposition for those pixels only, for which the charge deposition exceeds a certain threshold.

The spatial resolution of the telescope system was measured using the residuals between the position determined from the DUT data and the extrapolation to the DUT plane of the tracks fit to the strip data. For this purpose, the relative alignment of the DUT to the strip planes is calculated. Events with a χ^2 -probability of the track fit greater than 0.02 were selected from data taken with the beam along the normal to the pixel plane. In figure 15, the residuals along the short ($50 \mu\text{m}$) pixel cell direction are shown for events, for which only one pixel reported a hit (upper histogram) and events, for which two neighboring pixels reported a hit (lower histogram). The reconstructed position on the DUT of the single pixel hits is the centre of the hit pixel cell, while for two pixel hits an interpolation algorithm is used to determine the hit position using the charge deposition information [10,11]. The latter distribution can be used to give an estimation of the telescope resolution.

A gaussian fit to the two pixel residual distribution yields $\sigma = 5.5 \mu\text{m}$. This is the convolution of the telescope resolution and the pixel detector intrinsic resolution. The latter can be estimated as follows. As tracks are uniformly distributed, the width L of the region in which charge division between two pixels occurs can be estimated using the ratio between the number of two pixel and one-pixel hits. This yields $L \simeq 10 \mu\text{m}$. The expected r.m.s. of the residual distribution for these tracks is $\sigma = L/\sqrt{12} = 2.9 \mu\text{m}$. Thus, the width of the actual residual distribution is dominated by the telescope resolution, which can be estimated conservatively to be better than $\sigma = 5.5 \mu\text{m}$ in the DUT plane.

8 Summary

A high speed modular PC based beam telescope using double sided silicon microstrip detectors with on module data preprocessing has been built and successfully taken into operation. Telescope hard- and software are capable of stand-alone operation and easy to handle; integration of an additional "device under test" is straightforward. Pedestal subtraction, hit detection and zero suppression are done inside every module, reducing the data volume by a factor of 1/80. With its two level data acquisition scheme, the system can process event rates up to 7.6 kHz. The telescope is a factor of 75 (40) [2] ([1]) faster than conventional VME based systems while providing comparable

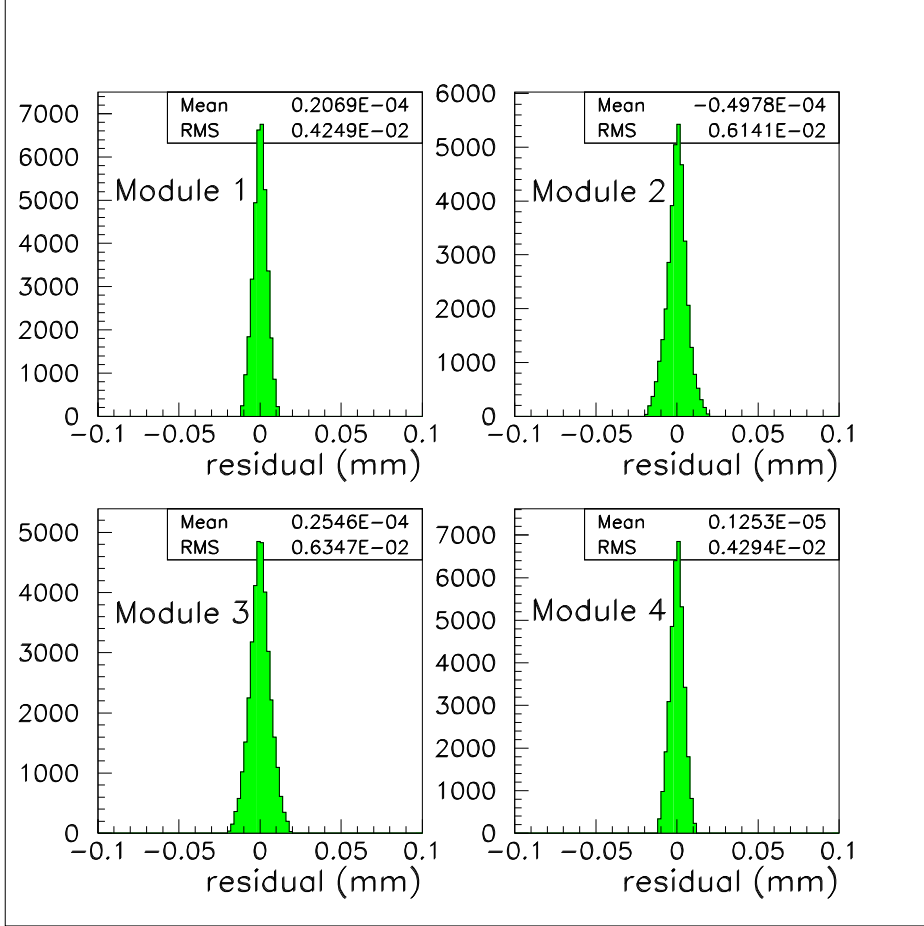


Fig. 14. Residual distributions between the strip hits and the fitted track.

performance. Signal to noise ratios of up to 70 were achieved. The spatial resolution in the DUT plane has been determined to be better than $5.5 \mu\text{m}$.

Acknowledgements

We gratefully acknowledge the help obtained from Walter Ockenfels and Ogmundur Runolfsson when encountering problems concerning mechanics, case design and handling and bonding of silicon detectors. We would also like to thank the members of the ATLAS pixel collaboration, in particular John Richardson from LBNL, Berkeley, and Attilio Andreazza, Francesco Ragusa and Clara Troncon from the Milano ATLAS group, for providing help and know-how in testbeam data taking and data analysis.

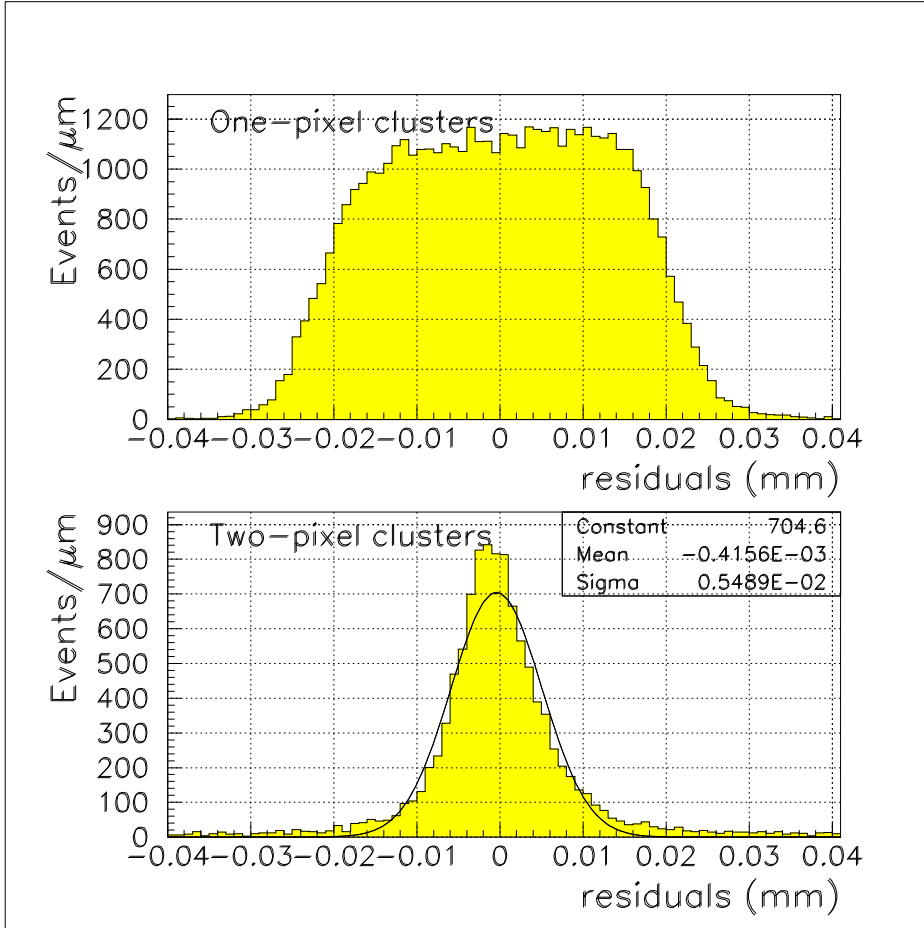


Fig. 15. Residual distributions between the pixel hits and the extrapolation of the track to the pixel detector plane along the short direction of the pixel cell. The upper histogram is for single pixel clusters, the lower histogram for two pixel clusters with a gaussian fit superimposed.

References

- [1] C. Eklund et al., Nucl. Instr. and Meth., A 430, (1999) 321.
- [2] P. Fischer et al., Nucl. Instr. and Meth., A 364, (1995) 224.
- [3] L.Celano et al., CERN-PPE/95-106, CERN, Geneva (1995).
- [4] Catalog *Si photodiodes and charge sensitive amplifiers for scintillation counting and high energy physics*, Published by Hamamatsu, catalog number KOTH00020E05 (1997).
- [5] *The VA 2. Specifications & Manual. Version 1.4.* Published by IDE AS, Oslo, Norway (1997).
- [6] *BELLE SVD hybrid. Conceptual design report. Version 2.3.* Published by IDE AS, OSLO, Norway. (1997).

- [7] Bjørn Magne Sundal, *Technical design report for BELLE SVD readout hybrid*. Published by IDE AS, OSLO, Norway. (1997).
- [8] *BB-PCI 20*. PCI Interface-Karte für das BlueBoard ASIC Testsystem. Documentation. Published by Silicon Solutions, Bonn (1999).
- [9] E. Belau et al., Nucl. Instr. and Meth., A 214, (1983) 253.
- [10] T. Lari, Nucl. Instr. and Meth., A 465 (2001) 112-114.
- [11] T.Lari, *Study of silicon pixel sensors for the ATLAS detector*, CERN-THESIS-2001-028, CERN, Geneva (2001).
- [12] N. Wermes for the ATLAS pixel collaboration, *Designs and prototype performance of the ATLAS pixel detector*, BONN-HE-99-07, Bonn (1999).
- [13] Alam M.S. et al., Nucl. Instr. and Meth., A 456, (2001) 217.